RESEARCH ARTICLE | Nutrient Sensing, Nutrition, and Metabolism

Small adipose stores in cystic fibrosis mice are characterized by reduced cell volume, not cell number

Ilya Bederman,¹ Alex DiScenna,¹ Leigh Henderson,² Aura Perez,¹ Jeannie Klavanian,² Daniel Kovtun,¹ Olivia Collins,¹ John Dunn,¹ Bernadette Erokwu,³ Christopher A. Flask,^{3,4} and Mitchell L. Drumm^{1,2}

¹Department of Pediatrics, Case Western Reserve University, Cleveland, Ohio; ²Department of Genetics and Genome Sciences, Case Western Reserve University, Cleveland, Ohio; ³Department of Radiology, School of Medicine, Case Western Reserve University, Cleveland, Ohio; and ⁴Department of Biomedical Engineering, School of Engineering, Case Western Reserve University, Cleveland, Ohio

Submitted 30 March 2017; accepted in final form 5 September 2018

Bederman I, DiScenna A, Henderson L, Perez A, Klavanian J, Kovtun D, Collins O, Dunn J, Erokwu B, Flask CA, Drumm ML. Small adipose stores in cystic fibrosis mice are characterized by reduced cell volume, not cell number. Am J Physiol Gastrointest Liver Physiol 315: G943-G953, 2018. First published September 6, 2018; doi:10.1152/ajpgi.00096.2017.—Cystic fibrosis (CF) is a lethal genetic disorder that affects many organ systems of the body, including various endocrine and exocrine tissues. Health and survival positively associate with body mass, and as a consequence, CF clinical care includes high-fat, high-calorie diets to maintain and increase adipose tissue stores. Such strategies have been implemented without a clear understanding of the cause and effect relationship between body mass and patients' health. Here, we used CF mouse models, which display small adipose stores, to begin examining body fat as a prelude into mechanistic studies of low body growth in CF, so that optimal therapeutic strategies could be developed. We reasoned that low adiposity must result from reduced number and/or volume of adipocytes. To determine relative contribution of either mechanism, we quantified volume of intraperitoneal and subcutaneous adipocytes. We found smaller, but not fewer, adipocytes in CF compared with wildtype (WT) animals. Specifically, intraperitoneal CF adipocytes were one-half the volume of WT cells, whereas subcutaneous cells were less affected by the Cftr genotype. No differences were found in cell types between CF and WT adipose tissues. Adipose tissue CFTR mRNA was detected, and we found greater CFTR expression in intraperitoneal depots as compared with subcutaneous samples. RNA sequencing revealed that CF adipose tissue exhibited lower expression of several key genes of adipocyte function (Lep, Pck1, Fas, Jun), consistent with low triglyceride storage. The data indicate that CF adipocytes contain fewer triglycerides than WT cells, and a role for CFTR in these cells is proposed.

NEW & NOTEWORTHY Adipocytes in cystic fibrosis mice exhibit smaller size due to low triglyceride storage. Adipocyte cell number per fat pad is similar, implying triglyceride storage problem. The absence of CFTR function in adipose tissue has been proposed as a direct link to low triglyceride storage in cystic fibrosis.

INTRODUCTION

http://www.ajpgi.org

Lack of energy stores has long been considered to be a clinically important feature of cystic fibrosis (CF), and treat-

Address for reprint requests and other correspondence: I. Bederman, Dept. of Pediatrics, Case Western Reserve Univ., 10900 Euclid Ave., BRB 715, Cleveland, OH, 44106-4948 (e-mail: ilya@case.edu).

ment has focused largely on increasing caloric intake. Specifically, high-fat, high-calorie diets, combined with pancreatic enzyme replacement therapy, have been used to compensate for the absence of exocrine pancreatic function and improve nutritional status of the patient. However, dyslipidemia of complex etiology is prevalent in CF patients (24), indicating that dietary lipids are not stored in adipose tissue, resulting in prevalent hypertriglyceridemia. Adipose tissue plays an important role in balancing daily lipid flux, i.e., storing triglycerides during times of excess and releasing fatty acids and glycerol as energy needs rise (7). Low adipose tissue limits energy capacity of an organism, thus affecting life functions. The occurrence of chronic infections and inflammation, which are prevalent in CF patients, may be affected by the low energetic capacity of insufficient energy stores. Stallings et al. (29), recently showed that Ivacaftor treatment improved body weight and adiposity of CF patients consuming high-fat, highcalorie diets via proposed mechanisms of lowered energy expenditure, gut inflammation, and fat malabsorption. This study highlights the complex etiology of low growth and adiposity in CF patients. Although body weight and composition of CF patients improved, it is not clear what other tissues were affected by the Ivacaftor treatment, for example, activation of adipose tissue cystic fibrosis transmembrane conductance regulator (CFTR) that allowed for lipid accretion. Thus, the potential role of adipose tissue CFTR needs further consideration.

Animal models of CF also experience reduced body mass and length, supporting their suitability for studying CF-related growth deficiency. The mouse is of particular interest, as it displays reduced growth while maintaining a significant level of exocrine pancreatic function (10), and in our colonies, intestinal fat malabsorption is not apparent with standard rodent chow (1). Use of conditional Cftr alleles demonstrated that gastrointestinal function is not responsible for the growth manifestations of CF (9), suggesting that they are not simply consequences of malnourishment alone. We previously reported that CF mice exhibit 1) significant suppression of the growth axis due to endocrine disruption (27), 2) low hepatic de novo lipogenesis and fatty acid elongation (1), and 3) elevated energy expenditure (6), with all contributing to low growth and lack of adipose tissue storage. To overcome low de novo lipogenesis and following CF patient recommendation of highfat diet feeding, we fed CF mice a high-fat diet. We recently reported that high-fat diet feeding failed to improve growth and adiposity in CF mice (2). These observations suggest that the paucity of adipose tissue might be a consequence of multiple factors, such as poor substrate availability either from de novo pathways (via VLDL delivery) or chylomicron origin from intestinal absorption and/or developmental or other endocrine factors.

If nutritional intervention is to be optimal, it is important to understand the source of growth perturbations and adipose storage deficits in CF, as the appropriate treatments of these traits would be very different if not simply due to insufficient caloric intake. Thus, we questioned whether CF adipose tissue is characterized by low number of adipocytes or smaller-size adipocytes. In this work, we characterized white adipose tissue from CF mice to begin to understand how it is affected in CF and to generate testable hypotheses for understanding the mechanisms involved. We found that CF fat depots are smaller due to reduced cell triglyceride content and that this was not due to infiltration of inflammatory cells or the presence of other cell types. Growth of visceral and subcutaneous white adipose tissue was not affected equally by the absence of Cftr. We used RNA analyses, transcriptome profiling, and quantitative RT-PCR to confirm that CFTR is expressed in white adipose tissue and mature adipocytes.

MATERIALS AND METHODS

Mice and Husbandry

Mouse care and experimental procedures were carried out in accordance with Case Western Reserve University Institutional Animal Care and Use Committee-approved protocols. All animals were congenic on a C57BL/6J background (>20 generations backcrossing). Sex- and age-matched homozygous wild-type (WT) littermates (Cftr^{+/+}) served as WT controls. All CF mice were offspring of Cftr heterozygotes (Cftr^{tm1Kth/+}). Mice were housed at a constant temperature (22°C) on a 12-h:12-h light-dark cycle alternating at 0600 and 1800. All mice were weaned at 28 days of age and allowed unrestricted access to chow and sterile water with Colyte (5). Mice were euthanized by exsanguination.

Adipose Tissue DNA and Triglyceride Isolation

Whole epididymal fat pads from WT and CF 6- to 7-wk-old male mice (n = 12 for each genotype) were excised, blotted dry, and weighed. Each fat pad was then partitioned into triplicate samples (\sim 20–30 mg each), weighed, flash-frozen in liquid N_2 and stored at -80°C until use. The partitioned adipose tissue samples were homogenized in 1 ml of digestion buffer (100 mM NaCl, 10 mM Tris-Cl, 25 mM EDTA, 0.5% SDS, and 0.1 mg/ml proteinase K, pH 8), and DNA was extracted by the addition of 1 ml of chloroform. Samples were vortexed and centrifuged at 14,000 rpm (5 min, 4°C) to separate the aqueous and organic layers. The upper aqueous layer containing nucleic acids was removed, and the remaining organic layer was preserved for triglyceride analyses and stored at -80°C. DNA was precipitated by the addition of 0.1 vol of 3 M sodium acetate (pH 5.2) and 2 vol of ice-cold ethyl alcohol and frozen at -80° C for 15 min. DNA was allowed to thaw, vortexed, and centrifuged at 14,000 rpm (10 min, room temperature). The resulting DNA pellet was washed twice with 200 µl of 70% ethyl alcohol, vortexed, and centrifuged. The pellet was allowed to dry and then resuspended in 25 µl of DNAse-free water. DNA concentration was determined using the Quant-iT PicoGreen dsDNA (Invitrogen, Carlsbad, CA), fluorescence-based assay, following the manufacturer's recommendations.

DNA concentration was normalized to the weight of adipose tissue (mg/g tissue). The preserved organic layer containing triglycerides was evaporated, and triglycerides were hydrolyzed by the addition of 0.5 ml of 1 N KOH (70% ethyl alcohol, vol/vol) at 90°C for 1 h. Samples were acidified by the addition of 150 µl of 12 N HCl, and triglyceride-bound fatty acids were removed by hexane extraction and discarded. The remaining aqueous sample containing triglyceride-bound glycerol was evaporated to dryness in Savant SpeedVac (Thermo Fisher Scientific, Waltham, MA) and reconstituted in 1 ml of water and adjusted to pH 7. Glycerol concentration was determined using Free Glycerol Reagent (Sigma, St. Louis, MO), following the manufacturer's instructions.

Histological Analysis

Adipocyte counting by hematoxylin and eosin staining. Gonadal adipose tissue was excised from 6- to 7-wk old WT and CF mice (n =12 for each genotype). The excised tissue was fixed for 24 h in 10% formalin, washed, stored in 70% ethanol, and then embedded in paraffin. Tissue paraffin blocks were sectioned at 7 µm and placed three to a slide. Analyzed sections were 125 µm apart to prevent counting a given adipocyte twice. Next, tissue section paraffin was removed in xylene and rehydrated through graded ethanol. Sections were then stained with hematoxylin and eosin to assess morphology. Slides were scanned at ×40 magnification in bright-field mode on a SCN400 Slide Scanner (Leica, Wetzlar, Germany). High-resolution images were analyzed using Visiopharm software (Visiopharm, Hoersholm, Denmark) to view and count adipocytes. The researchers were blinded to the sample genotypes and chose three random fields. A total of five independent operators evaluated repeated cell counts, which were normalized to the magnification and the area of field used and averaged.

Adipocyte cross-sectional area by immunohistochemistry. Epididymal and interscapular adipose tissues were excised from 6- to 7-wk-old WT and CF male mice (n = 6 for each genotype). From each animal, three slides with three adipose tissue sections were prepared as above. Sections were permeabilized with 0.3% Triton-X in PBS for 20 min, and antigens were retrieved with a 90°C, 10 mM sodium citrate bath for 20 min. Cooled sections were blocked with 5% donkey serum and 1% BSA for 1 h. Sections were then incubated with anti-perilipin A antibody (Ab3526; Abcam, Cambridge, MA), marking the lipid droplet membrane, at 1:500 overnight at 4°C. After washing, sections were incubated with secondary antibody conjugated to Alexa Fluor 594 (Ab150076; Invitrogen, Carlsbad, CA) at 1:500 for 2 h at room temperature. Negative controls were run by either omitting the primary antibody or both antibodies; nonspecific staining was not observed. Coverslips were applied using Vectashield mounting medium containing DAPI (Vector Laboratories, Burlingame, CA). Whole slides were scanned at ×40 magnification in fluorescent mode on a SCN400 Slide Scanner. For each tissue slice, three 439.22 × 334.25-µm fields were manually cropped and saved as separate images using the Leica SCN400 Image Viewer program.

Adipocyte area quantification (automated macro-based method). The resulting images were analyzed utilizing the freely available software package ImageJ (version 1.50d; http://imagej.nih.gov), similar to methods reported by others (20). Specifically, we developed a two-part ImageJ macro (see scripts below) that quantifies the area within lipid droplet membranes stained for perilipin A. Lipid droplet diameters were extrapolated from the area by converting the area to that of a circle. First, an image containing perilipin A-stained adipose tissue was opened in ImageJ. Then the first macro was run, and it applied a threshold to produce a black and white image. Occasional folds or tears in lipid droplet membranes were manually corrected with the paintbrush tool after the original image was compared with the black and white image. Next, the second macro was run, and it used the "analyze particle" feature of ImageJ to detect and measure the area of lipid droplets. Lipid droplets that touch the border of the

image were excluded. The first output was an image containing a numbered outline of each assessed lipid droplet. This image was examined to ensure quality. The second output was the quantitative result, i.e., the area of each numbered lipid droplet. Results were then exported to Microsoft Excel for further manipulation. The scale, threshold, and range of detection were optimized for our conditions, as shown within the macro scripts:

```
MACRO 1
run("Set Scale...", "distance=4 known=1 pixel=1 unit=um global");
run("Set Measurements...", "area display redirect=None decimal=2");
dirInput = getDirectory("Choose Directory");
dirOutput = getDirectory("Choose Directory");
list = getFileList(dirInput);
setBatchMode(true);
for (i=0;i \le list.length;i++) {
  open(dirInput+ list[i]);
  run("8-bit");
  setAutoThreshold("Huang"):
  run("Convert to Mask");
  run("Options...", "iterations=5 count=1 pad edm=8-bit do=Open");
  saveAs("Jpeg", dirOutput + File.nameWithoutExtension + " Threshold");
  close(): }
 MACRO 2
run("Set Scale...", "distance=4 known=1 pixel=1 unit=um global");
run("Set Measurements...", "area display redirect=None decimal=2");
dirInput = getDirectory("Choose Directory");
dirOutput = getDirectory("Choose Directory");
list = getFileList(dirInput);
setBatchMode(true);
for (i=0;i < list.length;i++) {
  open(dirInput+ list[i]);
  setAutoThreshold("Huang");
  run("Convert to Mask");
  run("Analyze Particles...", "size=3-8000 circularity=0.30-1.00 show=
  Outlines display exclude summarize");
```

RNA Analyses

Isolation of mature adipocytes. Epididymal fat pads were excised from 6- to 7-wk old mice (n=4/genotype) and minced finely with scissors. Tissue was transferred to buffer containing 2 mg/ml collagenase, Type I (C2139; Sigma), and incubated at 37°C in a rotating shaker at 125 rpm for 1 h. Digestion was stopped by the addition of DMEM-F-12 medium (ThermoFisher Scientific). After centrifugation at 200 g for 10 m, adipocytes were concentrated at the top, and stromal vascular cells formed a pellet at the bottom. The adipocyte layer was carefully aspirated to a new tube. Isolated adipocytes were then spun down and washed three more times. Adipocytes were filtered from undigested tissue using a 70- μ m cell strainer (BD Falcon, Franklin Lakes, MD). The filter was washed through twice with media containing 2% BSA. Cell suspension was then centrifuged at 700 g for 10 m and re-suspended in fresh DMEM-F-12 media.

CFTR mRNA quantification. Total RNA was extracted with Qiazol Lysis Reagent (Qiagen, Valencia, CA), cleaned up using the RNeasy Mini Kit (Qiagen), and eluted in 30 μl of RNase-free water (Qiagen). RNA quality and concentration were assessed spectrophotometrically using a Nanodrop ND-1000 (NanoDrop Technologies, Wilmington, DE). cDNA was generated from 1 μg of RNA by reverse transcription using the qScript cDNA synthesis kit (Quanta Biosciences, Beverly, MA). Real-time quantitative PCR was performed on a StepOne PCR system (Applied Biosystems, Foster City, CA). CFTR mRNA expression was assessed via a TaqMan expression assay (Mm00445197_m1; Applied Biosystems) and normalized to the expression of the house-keeping gene β-actin (4352341E; Applied Biosystems). RNA was run

as a negative control for DNA contamination and experimental error. All TaqMan assays were run singleplex in triplicate. Fluorescence thresholds were manually set in the exponential phase of amplification, and the resulting cycle thresholds were averaged per triplicate. All tissues from one mouse were run on a single plate with a standard curve to determine reaction efficiency and avoid interassay variation. The standard curve was calculated from the amplification of five serial twofold dilutions of cDNA. Relative gene expression was calculated using the Pfaffl method (22) for normalization to the lung *CFTR* mRNA

RNA-seq. Total RNA from epididymal fat was isolated from 6- to 7-wk old WT and CF animals (n = 3 for each genotype) with Qiazol Lysis Reagent (Qiagen), cleaned -up using the RNeasy Mini Kit (Qiagen), and eluted in 30 µl of RNase-free water (Qiagen). RNA-seq libraries were generated using TruSeq stranded Total RNA Ribo-Zero mouse gold kit (Illumina, San Diego, CA), and the quality of resulting libraries was assessed using Agilent 2100 Bioanalyzer (Agilent Technologies, Santa Clara, CA). Sequencing was carried out using an Illumina HiSeq 2500 Rapid Run flowcell -2×100 bp run. Trimming and filtering of the reads to remove adaptor sequences and low-quality nucleotides were performed using Trimmomatic (version 0.36). The filtered reads were aligned to the UCSC mouse genome mm10 as a reference using Bowtie2 (version 2.2.9) and Tophat (version 2.1.1) (13). Assembly of transcriptomes and quantification of their expression were performed using Cufflinks (version 2.2.1). Expression levels were expressed as fragments per kilobase of transcript per million mapped reads (FPKM). Statistical significance in differential gene expression between WT and CF epididymal fat samples was determined with Cuffdiff (version 2.2.1). Both P and q values were determined and defined as uncorrected P value of the test statistic and FDR-adjusted P value of test-statistic, respectively, as previously described (26, 31). Test-stat is the value of the test statistic used to compute significance of the observed change in FPKM. Data were further analyzed and visualized using CummeRbund run under the R package (version 3.3.1) (https://www.bioconductor.org/packages/release/bioc/html/cummeRbund.html). Functional classification of expressed genes was done with TIBCO Spotfire, using OmicsOffice tools for functional classification (Palo Alto, CA). The data discussed in this publication have been deposited in NCBI's SRA database and can be accessed via the following reviewer/collaborator link to metadata: ftp://ftp-trace.ncbi.nlm.nih.gov/sra/review/SRP102411_ 20180814_144023_305cf1fb13b9539dcd317a0354c9ed61. (Note: the above URL is valid for a minimum of 3 mo but may be removed any time thereafter. If you require access to the metadata after 3 mo, please email sra@ncbi.nlm.nih.gov for an updated link. The data will be released after publication is confirmed.

Magnetic Resonance Imaging

After weaning, mice were acclimated to the Case Center for Imaging Research facility for several days. Immediately prior to imaging, 4-wk-old WT and CF mice (n = 4 for each genotype) were weighed and anesthetized with 2-3% isoflurane in oxygen. The mice were then placed in a prone position within a Bruker Biospec 7T MRI scanner (Bruker Biospin, Billerica, MA). A 72-mm-diameter volume coil was used for excitation and signal detection to maximize the uniformity of the images. After localizer scans, a Relaxation Compensated Fat Fraction MRI acquisition and reconstruction process was used to generate quantitative fat fraction maps for each imaging slice. Briefly, three asymmetric echo spin MRI acquisitions were acquired (repetition time/echo time = 1,500 ms/20 ms, 17-25 coronal slices, resolution = 200 μ M \times 1,000 μ M, 2 averages). They were acquired with different echo shifts to allow separate fat and water images to be generated. Finally, a semiautomatic image analysis was performed to generate separate fat and water images for each imaging slice. Total fat volume and lean body volume were calculated from a compilation of the fat fraction images and each animal's weight. The fat fraction and water fraction images were then segmented to calculate the respective volumes of peritoneal and subcutaneous adipose tissues (12). After scanning at 4 wk, mice were allowed to recover for 2 wk, and scans were repeated at 6 and 8 wk of age.

Statistical Analysis

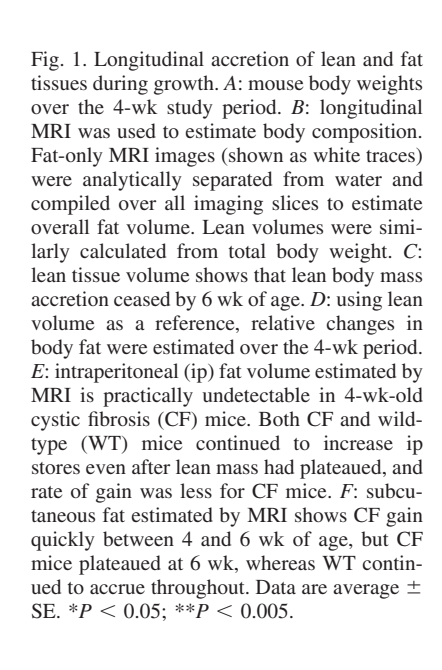
Data were presented as individual points as well as the average value. Group comparisons were performed by an independent two-tailed Student's *t*-test. Significance was accepted at P < 0.05.

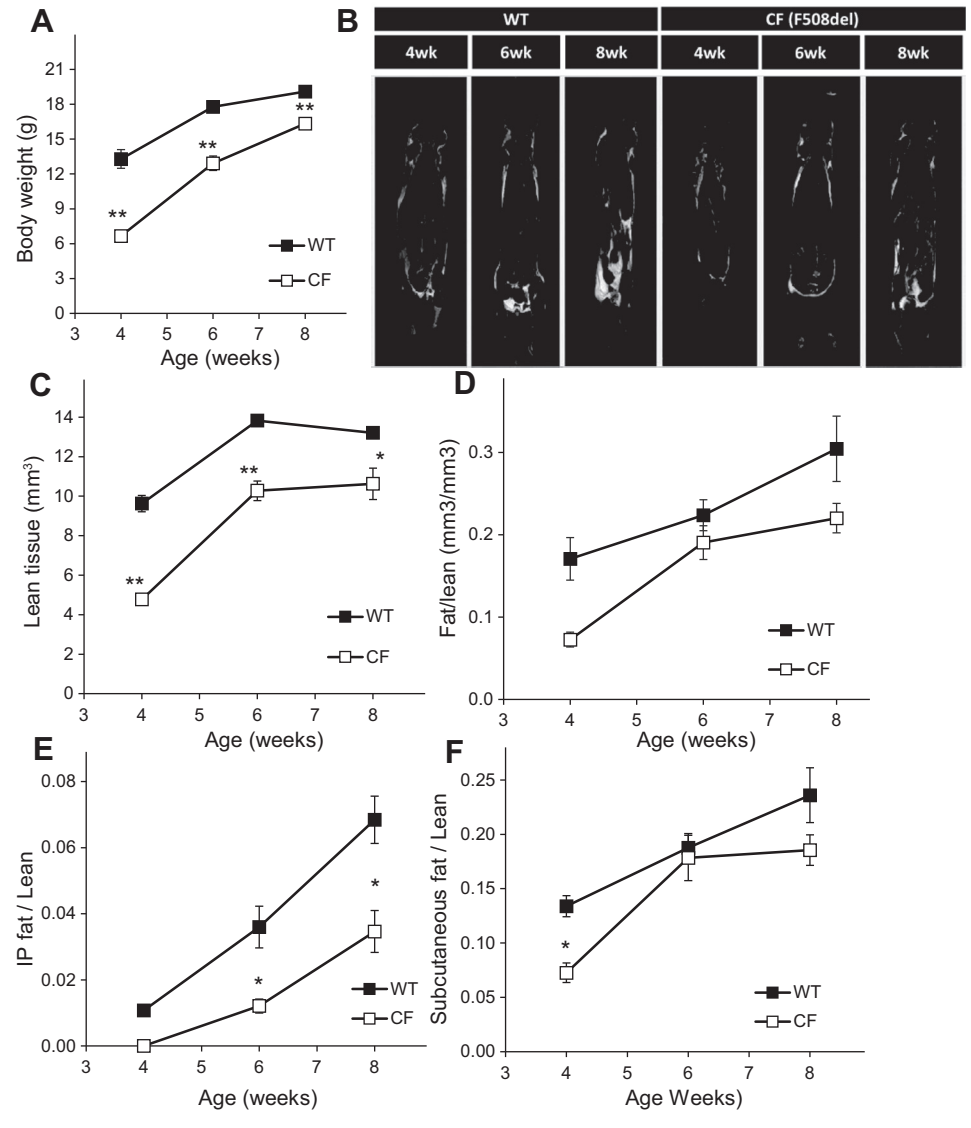
RESULTS

We and others previously showed that CF mice exhibit significantly lower bodily growth, body weight, length, and BMI. We also demonstrated that CF mice exhibit markedly decreased epididymal fat pads. These measurements represent a single time point, but body fat content is dynamic and changes with development and maturation, processes that are clearly delayed in CF. For the first time, we demonstrate age-dependent changes in body composition in addition to body weight changes (Fig. 1). Figure 1A shows time course of body weight during active growth (4–8 wk). It is evident that

CF mice exhibit "catchup" growth (body weight difference at 4 wk is \sim 2- to 1.3-fold at 8 wk). We examined age-related changes in body composition using magnetic resonance imaging (MRI) and assessed longitudinal changes in adipose stores of 4-, 6-, and 8-wk-old mice. Figure 1*B* shows images that captured changes in body fat (white outlines). Figure 1, C-F, shows changes in lean and various fat compartments, as quantified from the MRI images. MRI-derived estimates of whole body fat throughout the period studied (from 4 to 8 wk of age) confirmed that CF mice have less adipose tissue relative to lean mass. CF body fat did not appear to be shifted simply due to growth delay. WT mice appeared to accelerate fat accretion at 6 wk of age, whereas CF mice appeared to plateau.

White adipose tissue depots differ functionally by type and anatomic location, perhaps most notably between visceral and subcutaneous stores (16, 33). Even within a type of fat tissue, there is increasing evidence of distinct attributes, for example, distinct gene expression profiles between different subcutaneous depots (21). Differentiating between subcutaneous and intraperitoneal (visceral) fat and quantifying these compartments can also be done using MRI (4, 11). Intraperitoneal and





subcutaneous fat were quantified separately (Fig. 1, E and F) and, when referenced to both body weight and lean body mass, showed that fat accretion of the two compartments was quite different. The volume of both compartments increased over the 4-wk study period, but CF fat estimates were lower for both compartments at 4 wk of age, with subcutaneous plateauing at \sim 6 wk, whereas intraperitoneal continued to accumulate to 8 wk.

Small adipose tissue stores characteristic of CF could be explained by low cell number, cell volume, or both. An example of CF and WT epididymal fat pads in situ (Fig. 2A) shows markedly smaller CF fat pads compared with WT tissue from an age- and sex-matched animal. We measured directly

the number and size and calculated the volume of adipocytes from epididymal fat pads, representing the intraperitoneal compartment. To quantify size, epididymal fat pads were excised from 6-wk-old male mice and weighed. CF fat pads were, on average, about one-third of the weight of comparable tissue from WT mice (WT: 0.13 ± 0.01 vs. CF: 0.04 ± 0.01 g wet weight, P > 0.00001; Fig. 2B), but the weight of WT samples varied much more than those from CF mice. Normalized to the weight of the mouse, CF fat pads were about one-half the size of WT fat pads (not shown). The DNA and triglyceride contents of these fat pads were also measured to determine the cell number and size, respectively. No differences were detected in total DNA quantity (as normalized per entire fat pad;

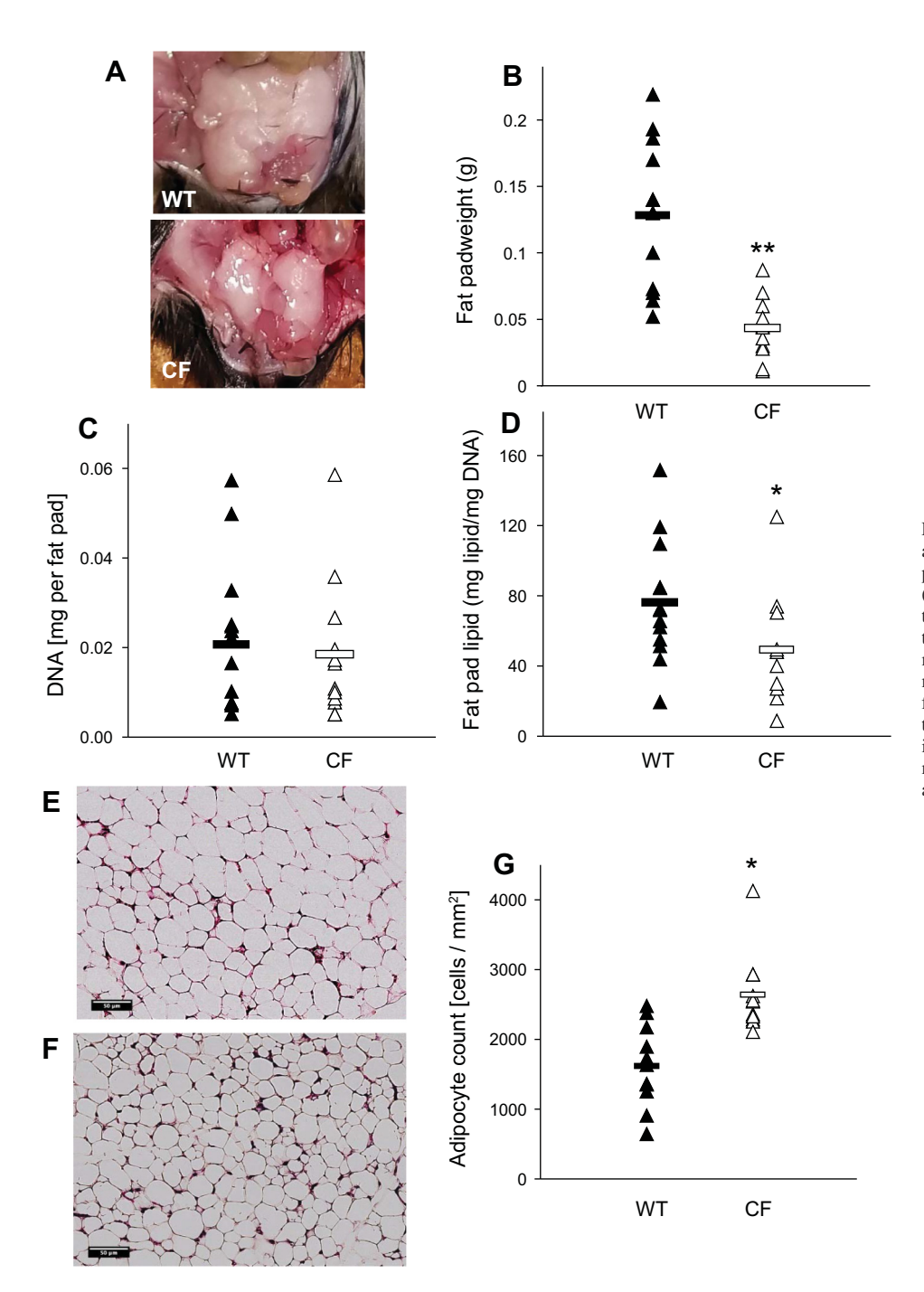


Fig. 2. Epididymal fat pad sizes, cell numbers, and contents. A: examples of epididymal fat pads from wild-type (WT) and cystic fibrosis (CF) mice. B: fat pad weights. C: DNA content/fat pad. D: triglyceride content normalized to DNA. E and F: histological staining of mouse adipose tissue (×40 magnification). Hematoxylin and eosin staining of intraperitoneal fat pad of WT (E) and CF (F) mice, respectively. G: cell density was estimated by counting cells per unit area. A, WT mice; A, CF mice. Dash symbol data point represents data average. *P<0.05; **P<0.005.

Fig. 2C) between CF and WT samples, indicating similar cell numbers in the entire respective fat pads. However, CF fat pad triglycerides were about one-half that of WT samples when normalized to DNA content (WT: 76.2 ± 9.6 vs. CF: 49.4 ± 9.2 mg lipid/mg DNA, P < 0.05; Fig. 2D).

Figure 2 data suggested that the number of cells in CF and WT fat pads was not different, but rather, the amount of triglyceride per cell was lower in CF. Because this could be due to a number of cellular differences (cell type, differentiation state, etc.), hematoxylin and eosin-stained sections of fat tissue from animals of both genotypes were examined, and tissues appeared qualitatively similar. Cell counting showed that there are 50% more cells per unit area in CF than WT tissue (WT: 1,616 \pm 161 vs. CF: 2,638 \pm 154 cells/mm², P < 0.0005; Fig. 2, E–G). This corresponds to a calculated volumetric difference of WT adipocytes being 2.08-times larger than CF adipocytes.

Because the accretion profiles of intraperitoneal and subcutaneous fat were different, we next examined examples of each for the differences in fat cell volume. Epididymal fat was used to represent visceral fat, and interscapular white adipose tissue was used to represented subcutaneous fat (28). Lipid droplets were stained with an antibody against the membrane protein perilipin A (Fig. 3, A–D, F, and G), and droplet cross-sectional areas were estimated. Diameters were calculated from the areas and plotted to compare the distribution of cell sizes (Fig. 3, E and H). The minimum and maximum cell sizes were very similar between CF and WT samples, but the distributions of the CF cells were shifted toward smaller-sized cells (Table 1). This shift was more apparent in the intraperitoneal cells than in the subcutaneous cells; this corresponded to WT cell volumes 96 and 34% greater, respectively, than CF cells in these two compartments. The calculated 96% difference in epididymal

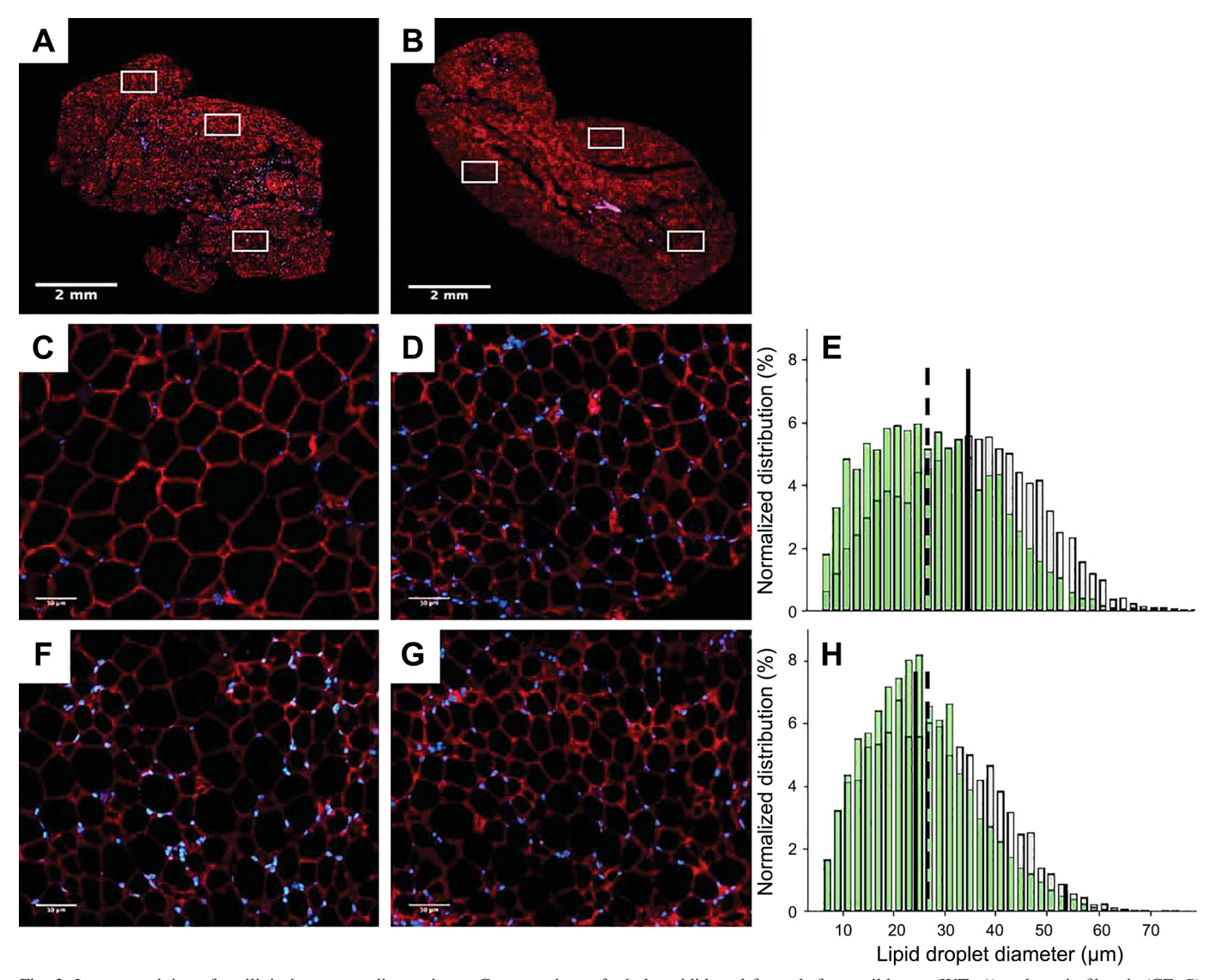


Fig. 3. Immunostaining of perilipin in mouse adipose tissue. Cross-sections of whole epididymal fat pads from wild-type (WT; A) and cystic fibrosis (CF; B) mice. C and D: boxes indicate randomly chosen fields for counting cell number and measuring areas depicted for WT (n = 3;975 cells; C) and CF (n = 5,777 cells; D). E: cell diameters for the epididymal fat were calculated and plotted as histograms. F-H: interscapular sections were analyzed for 6,009 WT (F) and 7,350 CF cells (G) and plotted similarly (H). For E and E, gray and green histogram profiles represent WT and CF samples, respectively. Vertical solid and dashed lines represent average lipid droplet counts for WT and CF samples, respectively.

Table 1. Normalized lipid droplet diameter distribution

		Lipid D	Proplet	Lipid Droplet Range				
Sample	n	Diameter, μm	Volume, µm ³	Minimum	Median	Maximum		
WT	3,975	34.61	21,700	6.00	34.89	78.22		
CF	5,777	27.71 (P < 0.0001)	$11,100 \ (\Delta = 1.96)$	6.02	26.66	71.68		
WT	6,009	27.81	11,200	6.05	26.98	68.22		
CF	7,350	$25.21 \ (P < 0.0001)$	$8,380 \ (\Delta = 1.34)$	6.00	24.15	74.20		

Top table shows intraperitoneal fat pad diameter distribution and bottom table shows subcutaneous fat pad diameter distribution. n is the total number of droplets measured (6 tissue samples were analyzed from each genotype). CF, cystic fibrosis; WT, wild type.

fat corresponded well with the 108% difference estimated from Fig. 2, E–G.

Reduced cell volume could be a consequence of less fatty acid uptake by CF cells or increased triglyceride catabolism. We previously showed that less newly synthesized, hepatic fatty acid was found in the adipocytes of CF than WT mice (1), consistent with less substrate uptake by CF adipocytes. As we found no evidence for the impaired intestinal fatty acid absorption, we wondered if the adipocytes themselves may be affected by CFTR's absence. Others have detected CFTR expression in white adipose tissue (19), providing the possibility that CF adipocytes are directly affected by the absence of CFTR.

We examined the utility of mouse models for this aspect of the human disease by measuring CFTR mRNA from a panel of murine tissues, including colon, lung, intraperitoneal (epididymal) fat, and subcutaneous fat, and compared relative expression to the same depots in humans from publicly available data (GTEx; http://www.gtexportal.org). The profiles from mouse tissues were very similar to those reported previously by others (19); however, subcutaneous fat was not included in that study. The profiles between mouse and human were strikingly similar (Fig. 4A), with the exception of subcutaneous fat, which was much lower in mouse than in human, relative to other tissues.

Additional white adipose tissue depots were examined, and CFTR mRNA was detected in all but interscapular fat (Fig. 4C). To determine whether the mRNA originated from the adipocytes or other cell types within fat tissue, mature adipocytes were separated from the stromal vascular cells and showed that adipocytes were the predominant source of CFTR mRNA signal. (Fig. 4C).

Adipose tissue macrophages have been implicated in contributing to reduced body fat content through suppressing differentiation of preadipocytes in lipodystrophies (15) and thus might explain the dystrophic CF adipose phenotype. Macrophage infiltration of adipose tissue was not observed during histological analyses for the presence of crown-like structures (17). RNA-seq-based transcriptome profiling provides a more sensitive analysis to detect differences in cell types or pathways that might be altered. For such comparisons, RNA was harvested from epididymal fat pads of mice (6–7 wk old), and transcriptome profiles were generated. As Fig. 5 shows, >29,762 transcripts were detected, and 1,785 of them were differentially expressed between WT and CF (P < 0.05). The distribution of genes that were increased or decreased between CF and WT tissue was very similar, 819 and 966, respectively.

The RNA-seq data were examined for evidence of changes in the proportions of cell populations and the differentiation

state of adipocytes. Transcript levels of various adipose markers reported by others (8, 18, 23) as signatures of stromal-vascular cells, preadipocytes, adipocytes, and macrophages are shown in Fig. 5B, along with *Cftr*. Genes associated with the adipocytes *Fabp4* (fatty acid-binding protein 4) and *Plin1* (perilipin) were highly expressed but not different between CF and WT samples. The adipokines leptin and adiponectin were also highly expressed, but leptin (*Lep*) was significantly lower in CF (approximately one-half of WT), and adiponectin trended in the same direction. As expression of these genes correlates to triglyceride content of adipocytes, these genes appeared to show predictable expression patterns.

Messenger RNAs from Pparg (encoding PPAR γ) and Cebpa (CREB enhancer-binding protein- α), genes involved in adipocyte differentiation, were compared and were not different. The only genes in the surveyed panel that appeared different were Jun, Cebpd, Lep, and Pck1. Jun and Cebpd are two transcription factors involved in early adipocyte differentiation (18). Lep gene encodes for leptin, a protein that plays a major role in the regulation of body weight and energy balance. Pck1 gene encodes cytosolic phosphoenolpyruvate carboxykinase, a key enzyme of glyceroneogenesis, i.e., generation of the glycerol-3-phosphate backbone for triglyceride storage in adipocytes (30). Additionally, Fas (fatty acid synthetase), which is responsible for de novo lipogenesis, was significantly decreased in CF mice. Decreased adipose tissue de novo lipogenesis rate indicates low carbohydrate availability and contributes to low lipid storage.

The presence of tissue macrophages was evaluated by the expression of the macrophage markers CD14 and ADGRE1 (encoding F4/80) (32). ADGRE1 was not different between CF and WT tissue, but CD14 mRNA was lower in CF tissue. The presence of macrophages in adipose tissue associates with obesity (32) and, therefore, fewer macrophages in CF adipose tissue is concordant with the reduced fat content in these animals. Nevertheless, our finding of less macrophage mRNA in CF tissue is interesting, as CF is considered a condition of chronic inflammation in which one might expect excessive macrophage infiltration.

DISCUSSION

Low body mass experienced by individuals with CF has historically been attributed to malabsorption and malnutrition. CF mice also display the low body mass phenotype without detectable malabsorption, indicating the involvement of additional factors. We previously showed (1) that low de novo lipogenesis in the liver and adipose tissue significantly contributed to low adipose tissue stores. These data suggested that low

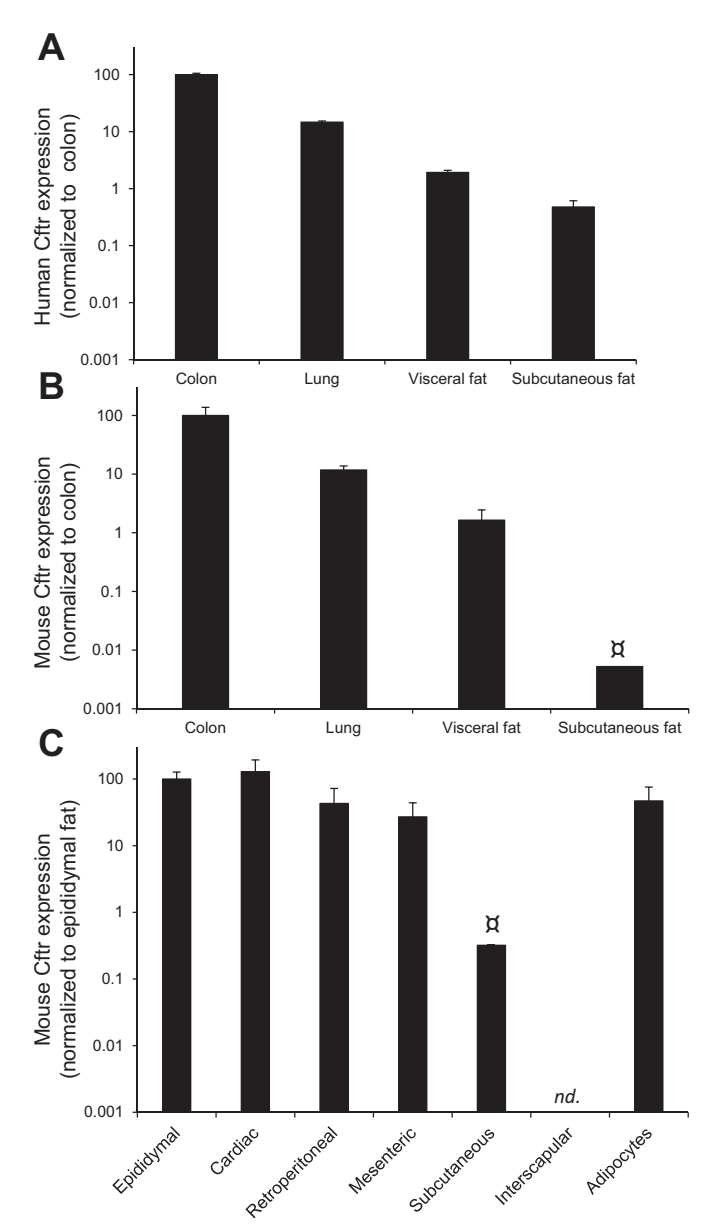


Fig. 4. In vivo and in vitro cystic fibrosis transmembrane regulator (Cftr) mRNA expression. A and B: RNA-seq profiles of human tissues (GTEX; A) were compared with mouse tissues (B) to examine relative expression levels. Human omental fat was the source of visceral adipose tissue. C: different murine adipose depots as well as mature isolated adipocytes were compared for Cftr mRNA by referencing to epididymal fat (n = 4). "Only 1 sample had detectable Cftr mRNA; nd, Cftr mRNA was not detectable.

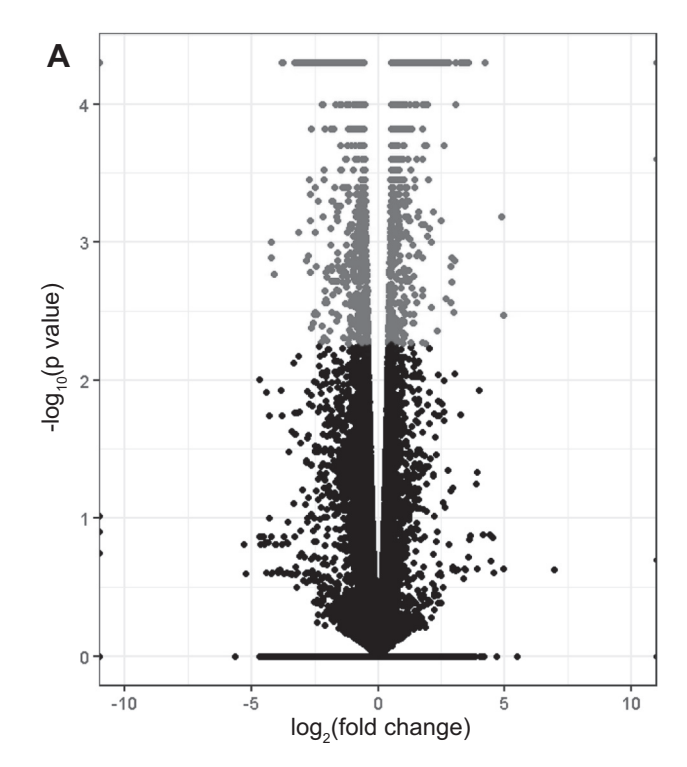
adipocyte volume may be the reason for overall low adipose tissue storage, not number of adipocytes. The work reported here tests whether low adipose tissue in CF mice is caused by low adipocyte number or low adipocyte volume. Our data indicate that white adipose tissue is smaller in CF because of cell volume rather than a reduction in adipocyte number. This volumetric difference varies between depots. Interscapular, subcutaneous WT adipocytes were estimated by histology to be 34% larger than CF cells, consistent with estimates of 31% by MRI for the entire body's subcutaneous depot. Similarly, WT adipocytes from epididymal fat, representing the visceral or intraperitoneal compartment, were estimated by histology to be

96% larger than CF cells, also consistent with MRI that estimates the entire intraperitoneal fat compartment to be 101% larger in WT animals. Such comparable results, obtained by two very different methodologies on independent groups of animals, strongly support our conclusions. Furthermore, the relative differences in subcutaneous versus visceral adipocyte sizes agree well with our recently published work (2), where we cross-bred CF mice with mice lacking leptin receptor signaling (db/db) in an attempt to overcome low food intake and de novo lipogenesis and high energy expenditure. CF mice carrying db/db mutation exhibited rapid expansion of subcutaneous $(7\times)$ and visceral $(14\times)$ adipose tissue depots, demonstrating the ability to accrue lipids under the conditions of abundant substrate. Still, CF db/db mice accumulated fewer lipids than db/db alone, indicating the remaining effect of missing CFTR signaling.

After determining that the difference in adipose stores is due to cell size, we reasoned that in addition to low triglyceride deposition, shown earlier, there may be high rates of lipolysis driven by tissue inflammation (25). We examined gene expression data for clues regarding the mechanism, particularly evidence of various cell types in different proportions between genotypes. We found no evidence for increased tissue macrophages by histology, nor was the expression of macrophage-specific genes different. Transcriptome profiles generated by RNA-seq were analyzed for evidence of different cell type proportions, but no such evidence was found. RNA-seq also confirmed CFTR expression in adipose tissue and provides a data set from which hypotheses about the mechanism can be developed.

From the adipocyte mRNAs that were different, *Jun*, *Cebpd*, *Lep*, and *Pck1* were all reduced in CF tissue and provided evidence for testable hypotheses. *Jun* and *Cebpd*, for example, may suggest differences in the differentiation of adipocytes (18). Lower *Lep* expression is consistent with lower triglyceride content of the cells we report here. We also found lower expression of the *Fas* (key enzyme of de novo lipogenesis) and *Pck1* genes [encoding phosphoenolpyruvate carboxykinase, a rate-limiting enzyme of glyceroneogenesis (30) in adipocytes]. These data together may indicate low glucose availability for de novo lipogenesis and an impairment of the adipocyte to generate glycerol-3-phosphate backbone needed for triglyceride synthesis, resulting in fewer stored triglycerides. This agrees with our *db/db* data, where excess carbohydrates were stored as triglycerides, as discussed earlier.

CFTR has been found in many nonepithelial cell types, but a unifying mechanism of growth regulation by CFTR has not been established. We propose that CFTR, a regulated anion channel, contributes to the maintenance of plasma membrane potential. In the adipocyte, this could affect other channels, such as the volume-regulated potassium channels involved in lipid metabolism, particularly fatty acid accretion through Glut4 regulation (14). This is needed for glucose entry to support de novo lipogenesis and to generate the glycerol-3phosphate triglyceride backbone. White adipose tissue samples isolated from rats were reported to have cAMP-stimulated chloride conductance (3), providing a possible link between CFTR and adipocyte function. Consistent with this hypothesis, we found little to no CFTR mRNA in subcutaneous fat, whereas it was readily detectable in intraperitoneal depots that appear to be affected to a greater extent by CFTR's absence in



4		•
l	L	,

	RNAseq	qPCR		
	Fold change	Fold change		
	(from WT)	(from WT)		
Lep	0.509	0.666*		
Pparg	1.258	1.422		
Adipoq	0.675	0.701		
Pck1	0.453	0.476*		

		CF mean	±	SD	WT mean	±	SD			
В	Adipose genes	FPKM			FPKM			Fold change	p value	q value
_	Мус	4.165	±	1.334	4.453	±	0.585	0.94	0.6675	0.9165
	Fos	3.273	±	1.167	3.520	±	1.395	0.93	0.6798	0.9213
	Jun	9.538	±	2.474	17.503	\pm	0.890	0.54	0.0001	0.0010
	Cebpb	7.869	\pm	1.240	12.802	\pm	2.797	0.61	0.0053	0.0488
	Cebpd	2.465	\pm	0.560	10.789	\pm	2.742	0.23	0.0001	0.0010
	Pparg	185.342	±	18.913	147.310	±	46.196	1.26	0.0680	0.2835
	Cebpa	222.663	±	36.994	218.426	±	60.676	1.02	0.8606	0.9726
	Vstm2a	0.082	±	0.054	0.051	±	0.047	1.62	1.0000	1.0000
	Zfp423	10.465	±	0.683	11.666	±	1.502	0.90	0.3072	0.6668
	Fabp4	11053.600	±	492.165	11477.400	±	947.454	0.96	0.9201	0.9832
	Adipoq	1240.400	±	111.236	1836.210	±	206.123	0.68	0.0215	0.1341
	Fas	10.462	\pm	1.157	16.924	\pm	3.295	0.62	0.0016	0.0185
	Plin1	574.803	±	59.485	556.969	±	87.697	1.03	0.8377	0.9688
	Lep	144.677	\pm	29.453	283.215	\pm	156.430	0.51	0.0001	0.0010
	Pck1	397.405	±	143.403	877.454	\pm	311.154	0.45	0.0001	0.0018
	Slc2a4	96.465	±	12.811	75.429	±	17.498	1.28	0.0128	0.0930
	Lpl	2050.100	±	328.124	1775.140	±	100.115	1.15	0.7196	0.9351
	Macrophage genes									
	Cd14	5.933	\pm	2.569	11.049	\pm	1.920	0.54	0.0002	0.0033
	Adgre1 Other	12.377	±	3.509	15.990	±	2.698	0.77	0.0171	0.1145
	Cftr	0.043	±	0.018	0.138	±	0.102	0.31	1.0000	1.0000

Fig. 5. Transcriptome profiling of cystic fibrosis (CF) and wild-type (WT) epididymal fat. A: each dot represents a transcript detected by RNA-seq. A total of 29,762 transcripts were detected, of which 1,785 were significantly different between CF and WT samples (gray dots). Of those, 966 were lower in CF than in WT (CF = 0.05–0.76 of non-CF) and 819 higher in CF (CF = 1.3–30 times greater than non-CF samples). B: mRNA values in fragments per kilobase of transcript per million mapped reads (FPKM) for selected genes. Genes in gray font were significantly different in CF samples as compared with WT. Statistical difference is represented by the P value (uncorrected P value) and Q value (FDR-adjusted Q value) of the test statistic (see MATERIALS AND METHODS). P: RT-Q-PCR replication of 4 genes selected from P (separate mice samples analyzed; P =

the mouse models. Furthermore, CFTR expression appears to be much greater in mature adipocytes than in the stromal-vascular fraction (data not shown), which contains the adipocyte precursor cells. This finding is consistent with increased chloride channel content, as adipocytes increase in size (3).

In conclusion, we ruled out that murine CF adipose tissue has low number of adipocytes. The lean body composition of CF mice and potentially CF patients is then explained by the low amount of stored triglycerides. Indeed, our CF mouse models exhibit inadequate delivery of dietary (high-fat diet failure) and/or de novo-made lipids, providing mechanistic insight of low triglyceride storage. The changes in gene expression signatures were consistent with the decreased activity of metabolic pathways involved in triglyceride formation and storage. We found that adipose tissue-specific Cftr mRNA was expressed mostly in adipocytes, although its direct role in adipose tissue is unknown. In our other work, we showed that when energy expenditure was low and lipids were in extreme excess, CF adipocytes were capable of storing triglycerides, which supports the importance of substrate availability. This finding suggests that Cftr is a potential modulator of lipid flux in adipocytes rather than a primary switch. Stallings et al (29) recently showed that Ivacaftor treatment resulted in body weight and adipose tissue gains in CF patients. They attributed the weight gain to improvements in gut inflammation, fat malabsorption, and decreased energy expenditure. Our CF mouse models do not exhibit gut inflammation or fat malabsorption; however, CF db/db mice exhibited marked gains of adipose tissue when energy expenditure was decreased and lipids were abundant. In addition to those mechanisms, we postulate that Ivacaftor may have activated adipose tissue Cftr, thus modulating lipid flux and resulting in lipid accumulation. Finally, we discussed only the influx of triglycerides; however, low adipose stores can also be caused by the inability to retain stored triglycerides via high lipolytic rates and free fatty acid-triglyceride cycling. These mechanisms will be examined in future experimentations.

ACKNOWLEDGMENTS

We acknowledge the use of the following core facilities at Case Western Reserve University: 1) the Histology Core (Department of Pediatrics), with technical assistance from Anjum Jafri; 2) the High Performance Computing Resource in the Core Facility for Advanced Research Computing; 3) the Genomics Core (Department of Genetics and Genome Sciences); and 4) the use of the Leica SCN400 Slide Scanner and the Visiopharm Image Analysis software in the Genetics Department Imaging Facility, sponsored by National Center for Research Resource (NIH-NCRR).

GRANTS

This work was supported by Shared Instrumentation Grant (1S10-RR-031845) as well as by grants from Cystic Fibrosis Foundation (BEDERM14G0 and DRUMM15R0). L. Henderson was supported by F31-HD-080320 from the National Institute of Child Health and Human Development.

The Genotype-Tissue Expression (GTEx) Project was supported by the Common Fund of the Office of the Director of the National Institutes of Health and by National Cancer Institute, National Human Genome Research Institute, National Heart, Lung, and Blood Institute, National Institute on Drug Abuse, National Institute of Mental Health, and National Institute of Neurological Disorders and Stroke. The data used for the analyses described in this manuscript were obtained from GTEx Portal (https://gtexportal.org/home/; access date: January 17, 2017).

DISCLOSURES

No conflicts of interest, financial or otherwise, are declared by the authors.

AUTHOR CONTRIBUTIONS

I.R.B., A.D., L.H., A.P., J.K., B.O.E., C.A.F., and M.L.D. conceived and designed research; I.R.B., A.D., L.H., A.P., J.K., D.K., B.O.E., and C.A.F. performed experiments; I.R.B., A.D., L.H., A.P., J.K., D.K., O.C., J.D., B.O.E., C.A.F., and M.L.D. analyzed data; I.R.B., A.D., L.H., A.P., J.K., D.K., O.C., J.D., B.O.E., C.A.F., and M.L.D. interpreted results of experiments; I.R.B., A.D., A.P., J.K., O.C., C.A.F., and M.L.D. prepared figures; I.R.B., A.D., L.H., A.P., J.K., C.A.F., and M.L.D. drafted manuscript; I.R.B., A.D., L.H., A.P., J.K., C.A.F., and M.L.D. edited and revised manuscript; I.R.B., A.D., A.P., J.K., C.A.F., and M.L.D. approved final version of manuscript.

REFERENCES

- Bederman I, Perez A, Henderson L, Freedman JA, Poleman J, Guentert D, Ruhrkraut N, Drumm ML. Altered de novo lipogenesis contributes to low adipose stores in cystic fibrosis mice. Am J Physiol Gastrointest Liver Physiol 303: G507–G518, 2012. doi:10.1152/ajpgi.00451.
- Bederman IR, Pora G, O'Reilly M, Poleman J, Spoonhower K, Puchowicz M, Perez A, Erokwu BO, Rodriguez-Palacios A, Flask CA, Drumm ML. Absence of leptin signaling allows fat accretion in CF mice. Am J Physiol Gastrointest Liver Physiol 315: G685–G698, 2018. doi:10. 1152/ajpgi.00344.2017.
- 3. **Bentley DC, Pulbutr P, Chan S, Smith PA.** Etiology of the membrane potential of rat white fat adipocytes. *Am J Physiol Endocrinol Metab* 307: E161–E175, 2014. doi:10.1152/aipendo.00446.2013.
- Berry DC, Stenesen D, Zeve D, Graff JM. The developmental origins of adipose tissue. *Development* 140: 3939–3949, 2013. doi:10.1242/dev. 080549
- Clarke LL, Gawenis LR, Franklin CL, Harline MC. Increased survival of CFTR knockout mice with an oral osmotic laxative. Lab Anim Sci 46: 612–618, 1996
- Darrah RJ, Mitchell AL, Campanaro CK, Barbato ES, Litman P, Sattar A, Hodges CA, Drumm ML, Jacono FJ. Early pulmonary disease manifestations in cystic fibrosis mice. *J Cyst Fibros* 15: 736–744, 2016. doi:10.1016/j.jcf.2016.05.002.
- Frayn KN. Adipose tissue as a buffer for daily lipid flux. *Diabetologia* 45: 1201–1210, 2002. doi:10.1007/s00125-002-0873-y.
- Gupta RK, Mepani RJ, Kleiner S, Lo JC, Khandekar MJ, Cohen P, Frontini A, Bhowmick DC, Ye L, Cinti S, Spiegelman BM. Zfp423 expression identifies committed preadipocytes and localizes to adipose endothelial and perivascular cells. *Cell Metab* 15: 230–239, 2012. doi:10. 1016/j.cmet.2012.01.010.
- Hodges CA, Grady BR, Mishra K, Cotton CU, Drumm ML. Cystic fibrosis growth retardation is not correlated with loss of Cftr in the intestinal epithelium. Am J Physiol Gastrointest Liver Physiol 301: G528– G536, 2011. doi:10.1152/ajpgi.00052.2011.
- Ip WF, Bronsveld I, Kent G, Corey M, Durie PR. Exocrine pancreatic alterations in long-lived surviving cystic fibrosis mice. *Pediatr Res* 40: 242–249, 1996. doi:10.1203/00006450-199608000-00009.
- Johnson DH, Flask CA, Ernsberger PR, Wong WC, Wilson DL. Reproducible MRI measurement of adipose tissue volumes in genetic and dietary rodent obesity models. *J Magn Reson Imaging* 28: 915–927, 2008. doi:10.1002/jmri.21481.
- Johnson DH, Narayan S, Wilson DL, Flask CA. Body composition analysis of obesity and hepatic steatosis in mice by relaxation compensated fat fraction (RCFF) MRI. J Magn Reson Imaging 35: 837–843, 2012. doi:10.1002/jmri.23508.
- 13. Kim D, Pertea G, Trapnell C, Pimentel H, Kelley R, Salzberg SL. TopHat2: accurate alignment of transcriptomes in the presence of insertions, deletions and gene fusions. *Genome Biol* 14: R36, 2013. doi:10. 1186/gb-2013-14-4-r36.
- Li Y, Wang P, Xu J, Desir GV. Voltage-gated potassium channel Kv1.3 regulates GLUT4 trafficking to the plasma membrane via a Ca2+dependent mechanism. *Am J Physiol Cell Physiol* 290: C345–C351, 2006. doi:10.1152/ajpcell.00091.2005.
- Liu LF, Craig CM, Tolentino LL, Choi O, Morton J, Rivas H, Cushman SW, Engleman EG, McLaughlin T. Adipose tissue macrophages impair preadipocyte differentiation in humans. *PLoS One* 12: e0170728, 2017. doi:10.1371/journal.pone.0170728.
- Meissburger B, Perdikari A, Moest H, Müller S, Geiger M, Wolfrum C. Regulation of adipogenesis by paracrine factors from adipose stromal-vascular fraction a link to fat depot-specific differences. *Biochim Biophys Acta* 1861: 1121–1131, 2016. doi:10.1016/j.bbalip.2016.06.010.

- Murano I, Barbatelli G, Parisani V, Latini C, Muzzonigro G, Castellucci M, Cinti S. Dead adipocytes, detected as crown-like structures, are prevalent in visceral fat depots of genetically obese mice. *J Lipid Res* 49: 1562–1568, 2008. doi:10.1194/jlr.M800019-JLR200.
- Ntambi JM, Young-Cheul K. Adipocyte differentiation and gene expression. J Nutr 130: 3122S–3126S, 2000. doi:10.1093/jn/130.12.3122S.
- Ollero M, Junaidi O, Zaman MM, Tzameli I, Ferrando AA, Andersson C, Blanco PG, Bialecki E, Freedman SD. Decreased expression of peroxisome proliferator activated receptor γ in CFTR^{-/-} mice. *J Cell Physiol* 200: 235–244, 2004. doi:10.1002/jcp.20020.
- Parlee SD, Lentz SI, Mori H, MacDougald OA. Quantifying size and number of adipocytes in adipose tissue. *Methods Enzymol* 537: 93–122, 2014. doi:10.1016/B978-0-12-411619-1.00006-9.
- Passaro A, Miselli MA, Sanz JM, Dalla Nora E, Morieri ML, Colonna R, Pišot R, Zuliani G. Gene expression regional differences in human subcutaneous adipose tissue. *BMC Genomics* 18: 202, 2017. doi:10.1186/s12864-017-3564-2.
- Pfaffl MW. A new mathematical model for relative quantification in real-time RT-PCR. *Nucleic Acids Res* 29: e45, 2001. doi:10.1093/nar/29. 9.e45.
- Radeau T, Robb M, McDonnell M, McPherson R. Preferential expression of cholesteryl ester transfer protein mRNA by stromal-vascular cells of human adipose tissue. *Biochim Biophys Acta* 1392: 245–253, 1998. doi:10.1016/S0005-2760(98)00039-3.
- 24. Rhodes B, Nash EF, Tullis E, Pencharz PB, Brotherwood M, Dupuis A, Stephenson A. Prevalence of dyslipidemia in adults with cystic fibrosis. *J Cyst Fibros* 9: 24–28, 2010. doi:10.1016/j.jcf.2009.09.002.
- Rittig N, Bach E, Thomsen HH, Pedersen SB, Nielsen TS, Jørgensen JO, Jessen N, Møller N. Regulation of Lipolysis and Adipose Tissue

- Signaling during Acute Endotoxin-Induced Inflammation: A Human Randomized Crossover Trial. *PLoS One* 11: e0162167, 2016. doi:10.1371/journal.pone.0162167.
- Roberts A, Trapnell C, Donaghey J, Rinn JL, Pachter L. Improving RNA-Seq expression estimates by correcting for fragment bias. *Genome Biol* 12: R22, 2011. doi:10.1186/gb-2011-12-3-r22.
- 27. **Rosenberg LA, Schluchter MD, Parlow AF, Drumm ML.** Mouse as a model of growth retardation in cystic fibrosis. *Pediatr Res* 59: 191–195, 2006. doi:10.1203/01.pdr.0000196720.25938.be.
- Sanchez-Gurmaches J, Hung CM, Guertin DA. Emerging complexities in adipocyte origins and identity. *Trends Cell Biol* 26: 313–326, 2016. doi:10.1016/j.tcb.2016.01.004.
- Stallings VA, Sainath N, Oberle M, Bertolaso C, Schall JI. Energy balance and mechanisms of weight gain with ivacaftor treatment of cystic fibrosis gating mutations. *J Pediatr* 201: 229–237.e4, 2018. doi:10.1016/ j.jpeds.2018.05.018.
- Tontonoz P, Hu E, Devine J, Beale EG, Spiegelman BM. PPAR gamma 2 regulates adipose expression of the phosphoenolpyruvate carboxykinase gene. *Mol Cell Biol* 15: 351–357, 1995. doi:10.1128/MCB.15.1.351.
- Trapnell C, Hendrickson DG, Sauvageau M, Goff L, Rinn JL, Pachter L. Differential analysis of gene regulation at transcript resolution with RNA-seq. *Nat Biotechnol* 31: 46–53, 2013. doi:10.1038/nbt.2450.
- Weisberg SP, McCann D, Desai M, Rosenbaum M, Leibel RL, Ferrante AW Jr. Obesity is associated with macrophage accumulation in adipose tissue. J Clin Invest 112: 1796–1808, 2003. doi:10.1172/ ICI200319246
- Wronska A, Kmiec Z. Structural and biochemical characteristics of various white adipose tissue depots. *Acta Physiol (Oxf)* 205: 194–208, 2012. doi:10.1111/j.1748-1716.2012.02409.x.

